Paleoceanography and Paleoclimatology

RESEARCH ARTICLE
10.1029/2018PA003467

Late Quaternary Biomass Burning in Northwest Africa and Interactions With Climate, Vegetation, and Humans

Laura T. Schreuder[1], Ellen C. Hopmans[1], Isla S. Castañeda[1,2], Enno Schefuß[3], Stefan Mulitza[3], Jaap S. Sinninghe Damsté[1,4], and Stefan Schouten[1,4]

[1]Department of Marine Microbiology and Biogeochemistry, NIOZ Royal Netherlands Institute for Sea Research, and Utrecht University, Den Burg, Netherlands, [2]Now at Department of Geosciences, University of Massachusetts Amherst, Amherst, MA, USA, [3]MARUM – Center for Marine Environmental Sciences, University of Bremen, Bremen, Germany, [4]Department of Earth Sciences, Faculty of Geosciences, Utrecht University, Utrecht, Netherlands

Key Points:
- Biomass burning history of sub-Saharan Northwest Africa during the last 192 kyr was studied, based on levoglucosan accumulation rates
- Glacial/interglacial changes in regional climate and vegetation composition were not a major influence on biomass burning
- Fire events around 50–60 ka in sub-Saharan Northwest Africa might be caused by increased fuel loads and human fire use

Supporting Information:
- Supporting Information S1
- Data Set S1

Correspondence to:
L. T. Schreuder,
laura.schreuder@nioz.nl

Citation:
Schreuder, L. T., Hopmans, E. C., Castañeda, I. S., Schefuß, E., Mulitza, S., Sinninghe Damsté, J. S., & Schouten, S. (2019). Late Quaternary biomass burning in Northwest Africa and interactions with climate, vegetation, and humans. *Paleoceanography and Paleoclimatology*, *34*, 153–163. https://doi.org/10.1029/2018PA003467

Received 22 AUG 2018
Accepted 6 JAN 2019
Accepted article online 9 JAN 2019
Published online 1 FEB 2019

Abstract Biomass burning on the African continent is widespread, and interactions with climate, vegetation dynamics, and biogeochemical cycling are complex. To obtain a better understanding of these complex relationships, African fire history has been widely studied, although mostly on relatively short timescales (i.e., years to kiloyears) and less commonly on long-term scales. Here we present a 192-kyr, continuous biomass-burning record from sub-Saharan Northwest Africa based on the fire biomarker levoglucosan in a marine sediment core offshore Guinea. Notable features of our record include an increase in levoglucosan accumulation at 80 ka and two peaks at 50–60 ka. The event at 80 ka is likely related to an overall increase in sedimentation rates rather than an increase in biomass burning in the Northwest African savanna region. Our record indicates that glacial/interglacial changes in regional climate and vegetation composition (C_3 vs. C_4 plants) were not a major influence on biomass burning over the last 192 kyr. However, we suggest that the burning events at 50–60 ka might be caused by increased occurrence of C_3 vegetation and human settlement in this region. At this time, the savanna region became wetter and fuel loads likely increased. Therefore, the region was more hospitable for humans, who likely used fire for hunting activities. Collectively, we hypothesize that on longer (glacial/interglacial) timescales, biomass burning, regional climate, and African vegetation are not necessarily coupled, while around 50–60 ka, higher fuel loads and human fire use may have influenced fire occurrence in sub-Saharan Northwest Africa.

1. Introduction

Biomass burning on the African continent is widespread and has long been recognized to influence biogeochemical cycling, vegetation dynamics, and climate (e.g., Bond & Keeley, 2005; Bowman et al., 2009). However, the interactions between fire, climate, and environment are complex and vary greatly across spatial and temporal scales (Whitlock et al., 2010). Fire is often discussed in terms of a fire regime, which describes its frequency, intensity, season, type, and extent (Bond & Keeley, 2005; Whitlock et al., 2010). Fire regimes are in turn dependent on climate, fuel, and landscape variables such as the amount and type of vegetation, ignition frequency (natural or human-induced), fuel wetness, and burning season (Whitlock et al., 2010). To obtain a better understanding of the controls on biomass burning and its complex interactions with climate, environment, and humans in Africa, fire regimes have been studied using satellites (Archibald et al., 2010) and historical data (Mouillot & Field, 2005). However, these studies only provide information on short-term (i.e., years to decades) changes in biomass burning and therefore do not capture the full range of fire variability in the ecosystem, which could lead to incomplete assumptions about the drivers and role of biomass burning in the ecosystem (Whitlock et al., 2010).

To reconstruct African fire history on longer time scales, sedimentary records of fire proxies have been used (e.g., Battistel et al., 2017; Dupont & Schefuß, 2018; Shanahan et al., 2016). One commonly used fire proxy is charcoal, which is a carbonaceous material produced by heating of biomass during incomplete combustion (Whitlock & Larsen, 2002) and is usually divided into two size classes: macroscopic charcoal (particles $\geq$ 100 μm) and microscopic charcoal (particles $\leq$ 100 μm). The smaller particles are assumed to be transported over longer distances compared to the larger particles, and therefore, macroscopic charcoal is usually used to reconstruct local-scale fires, while microscopic charcoal provides information on more

regional-scale fires (Marlon et al., 2016; Vachula et al., 2018). However, application of the charcoal proxy can sometimes be challenging. For example, there are many factors determining quantities of charcoal accumulating in sediments, such as the size of the deposition site or body of water, the type of vegetation burned, and combustion temperatures (Hawthorne et al., 2017, and references therein; Kuo et al., 2008). Another fire proxy is based on polycyclic aromatic hydrocarbons (PAHs), which can be formed during natural processes such as volcanic eruptions and biomass burning but can also originate from anthropogenic sources such as coal and wood burning, oil combustion and other industrial processes (Tobiszewski & Namieśnik, 2012, and references therein). Furthermore, PAHs can also be formed during diagenesis rather than combustion (e.g., Koopmans et al., 1996; Peters et al., 2005; Wakeham et al., 1980). PAHs are thus not solely formed during biomass burning, and therefore, PAH ratios have been mainly used to identify emission sources (Tobiszewski & Namieśnik, 2012; Yunker et al., 2002) and certain PAH ratios have been used as biomass-burning indicators in marine (Elias et al., 2001) and lacustrine (Miller et al., 2017) sediments.

One of the most specific biomass-burning proxies is levoglucosan (1,6-anhydro-β-D-glucose) and its isomers mannosan (1,6-anhydro-β-D-mannopyranose) and galactosan (1,6-anhydro-β-D-galactopyranose). These are thermal products of cellulose/hemicellulose combustion formed at a temperature range of 150–350 °C (Kuo et al., 2011; Shafizadeh et al., 1979; Simoneit et al., 1999). The amount of levoglucosan emitted during a fire event is dependent on burning conditions. Combustion temperature is the primary factor governing levoglucosan yield, while combustion duration has no significant effect (Kuo et al., 2008). The type of vegetation burned also influences levoglucosan yield and is related to variations in the cellulose and hemicellulose content across plant species and the presence of inorganic salts and lignin content in the plant tissue (e.g., Kuo et al., 2008, 2011; Simoneit et al., 1999). Nevertheless, levoglucosan is considered to be a robust tracer for biomass burning in aerosols because of its high emission and source-specificity (e.g., Simoneit & Elias, 2000) and has been used in numerous air-quality studies (e.g., Iinuma et al., 2016; Monteiro et al., 2018; Wang et al., 2007). Several studies have demonstrated that levoglucosan remains stable in the atmosphere for several days under most atmospheric conditions (Fraser & Lakshmanan, 2000; García et al., 2017; Hu et al., 2013; Mochida et al., 2003) and that levoglucosan can be transported through the atmosphere over hundreds of kilometers (e.g., Fu et al., 2011; Schreuder et al., 2018).

To date, biomass burning in Africa using sedimentary fire proxies has mostly been studied on relatively short timescales (i.e., years to kiloyears; e.g., Battistel et al., 2017; Dupont & Schefuß, 2018; Shanahan et al., 2016), while long-term fire dynamics are less commonly studied (e.g., Bird & Cali, 1998; Bird & Cali, 2002; Daniau et al., 2013). The latter are relevant as Africa, the continent where modern humans evolved, has the longest history of human fire use (Archibald et al., 2012). Furthermore, vegetation composition and climate on the African continent have markedly changed on glacial/interglacial timescales (Castañeda et al., 2009; deMenocal, 1995; Schefuß et al., 2003), which could influence biomass burning. It was recently shown for the tropical North Atlantic that levoglucosan is transported to the ocean floor by sinking particulate matter where it is preserved in surface sediments (Schreuder et al., 2018). This raises the potential to reconstruct the fire history of Africa on long (glacial to interglacial) timescales using marine sediment cores, which can provide long-term and continuous records.

Here we present a biomass-burning record from sub-Saharan Northwest Africa spanning the last 192 ka, based on the accumulation rates of levoglucosan in a sediment core from the Guinea Plateau Margin offshore West Africa (Figure 1, yellow star). This core has previously been studied for changes in vegetation and paleoceanography (Castañeda et al., 2009; Lopes dos Santos et al., 2010). Our new results shed light on biomass burning in sub-Saharan Northwest Africa and the complex interactions between fire, climate, vegetation, and human activity.

2. Material and Methods

2.1. Core Location and Age Model

Sediment core GeoB9528-3 was recovered from the Guinea Plateau Margin offshore West Africa at 09°09.96′ N, 17°39.81′W (Figure 1, yellow star) at 3,057-m water depth (Castañeda et al., 2009). The core has been previously shown to receive dust input from Northwestern Africa, where the modern vegetation zones are Mediterranean (C_3 dominated), Mediterranean-Saharan transitional (mixed C_3 and C_4 plants), Sahara desert (C_4 dominated), Sahel (mixed C_3 and C_4 plants, predominantly C_4 plants), Sudanian woodland

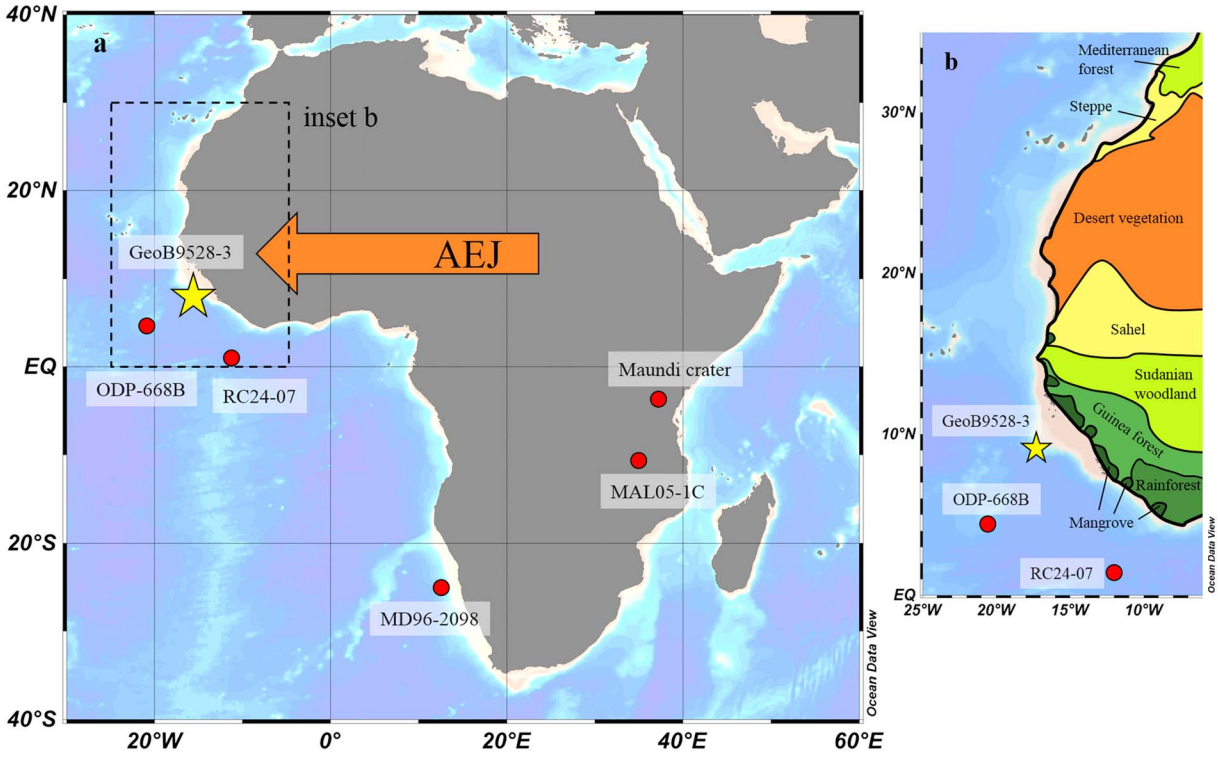

Figure 1. (a) Location of marine sediment core GeoB9528-3 offshore Guinea (yellow star) and other marine and lacustrine cores cited in this study (red dots). The African Easterly Jet (AEJ) is indicated with and orange arrow. (b) Zoom-in of Northwest Africa with modern vegetation belts on the continent, adapted from Kuechler et al. (2013). These maps were generated in Ocean Data View.

(mixed C_3 and C_4 plants), Guinean forest (mixed C_3 and C_4 plants, predominantly C_3 plants), and tropical rainforest (C_3 dominated; Figure 1b). The core site is today located near the transition from Guinean forest to Sudanian woodland (Figure 1b), where more C_4 vegetation reflects drier conditions (Castañeda et al., 2009; Kuechler et al., 2013). Terrestrial material from this region is transported offshore by the African Easterly Jet (AEJ). As previously discussed by Grousset et al. (1998), the direction of the AEJ likely remained constant during previous glacial and interglacial periods, and therefore, the core GeoB9528-3 provides a continuous record of environmental changes at the forest-woodland-savanna boundary in the Guinean area of sub-Saharan Northwest Africa.

The age model for core GeoB9528-3 is based on a graphic correlation of the benthic foraminifer *C. wuellerstorfi* $\delta^{18}O$ record (Castañeda et al., 2009) with the Deep North Atlantic Stack by Lisiecki and Stern (2016) and the global benthic stack by Lisiecki and Raymo (2005). Downcore age uncertainty was modeled with the R script BACON (Blaauw & Christen, 2011) version 2.2 using the 1-sigma age uncertainty assigned from the Deep North Atlantic Stack. BACON was run with default parameters and a student *t* distribution, with shape parameter (t.a.) of 10 and a scale parameter (t.b.) of 11. About 10,000 age-depth realizations were obtained to estimate the mean age and the standard deviation of the age ensemble at the sampling depth. Sedimentation rates were calculated using the depths and mean ages of the tie points.

2.2. Geochemical Analyses of Core GeoB9528-3

Sediment core GeoB9528-3 was sampled at 5-cm intervals for organic geochemical analyses. Sediment samples were freeze-dried, homogenized, and extracted with a DIONEX Accelerated Solvent Extractor (ASE 200) using a solvent mixture of 9:1 (v:v) dichloromethane (DCM):methanol (MeOH), as described previously by Castañeda et al. (2009).

2.2.1. Levoglucosan Analysis

A known amount (0.25 ng) of deuterated (D7) levoglucosan ($C_6H_3D_7O_5$; dLVG, from Cambridge Isotope Laboratories, Inc.) was added to aliquots of the total lipid extracts as an internal standard to quantify

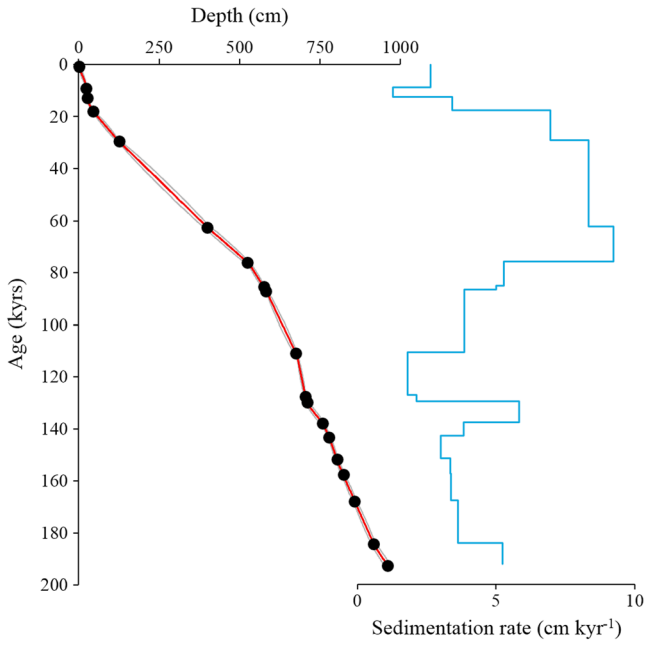

Figure 2. Age versus depth relationship as calculated for GeoB-9528-3 sediment core (red line) with 1σ error (grey line), plotted together with the tie points (black circles), and the corresponding sedimentation rates (blue line).

levoglucosan and its isomers, after which the extracts were dried under N_2. All extracts were redissolved in acetonitrile: H_2O (95:5, v:v) and filtered using a polytetrafluoroethylene filter (0.45 μm) before analysis. Levoglucosan and its isomers were analyzed by means of ultrahigh-performance liquid chromatography (UHPLC)-negative ion electro spray ionization/high resolution mass spectrometry (ESI/HRMS) using an Agilent 1290 Infinity UHPLC coupled to an Agilent 6230 time-of-flight mass spectrometer, as described previously (Schreuder et al., 2018). Separation was achieved with two Aquity UPLC BEH amide columns (2.1 × 150 mm; 1.7 μm, Waters Chromatography, at 30 °C) in series with a 50-mm guard column, and a mobile phase of acetonitrile, H_2O, and triethylamine (0.2 ml/min). The monitored mass range was m/z 150–350. Injection volume was usually 10 μl. Levoglucosan, its isomers, and dLVG were detected as their deprotonated molecules $(M\text{-}H)^-$. Quantification was based on peak integrations of mass chromatograms within 3-ppm mass accuracy using a calculated exact mass of 161.0445 m/z for levoglucosan ($C_6H_{10}O_5$) and its isomers and 168.0884 m/z ($C_6H_3D_7O_5$) for dLVG. Authentic standards for levoglucosan, galactosan, and mannosan were all obtained from Sigma Aldrich. Analytical performance and relative response factors for levoglucosan, galactosan, and mannosan compared to dLVG were determined daily by analysis of a standard mixture of levoglucosan, galactosan, mannosan, and dLVG and varied between 1.20 and 1.29 for levoglucosan, between 0.53 and 0.72 for galactosan, and between 0.86 and 1.04 for mannosan. Approximately 20% of the samples were analyzed in duplicate, which resulted in an average instrumental error of 4%.

2.2.2. Long-Chain *n*-Alkane Analysis

Analyses of the stable carbon isotope composition of long-chain *n*-alkanes were reported by Castañeda et al. (2009), while long-chain *n*-alkane quantifications will be described here. A known amount of squalane was added to aliquots of the extracts as an internal standard to quantify the plant leaf waxes (*n*-alkanes). The extracts were separated into apolar, ketone, and polar fractions via alumina pipette column chromatography using solvent mixtures of hexane/DCM (9:1, v:v), hexane/DCM (1:1, v:v), and DCM/MeOH (1:1, v:v), respectively. The apolar fractions were redissolved in hexane, and all samples were injected on-column with an Agilent 7890B gas chromatography instrument at 70 °C. The oven temperature was programmed to 130 °C at 20 °C/min, and subsequently to 320 °C (held 10 min) at 4 °C/min; He was the carrier gas at a constant 2 ml/min. Injection volume was 1 μl. The *n*-alkanes were quantified by integrating the peak area in the chromatogram and relating that to the peak area of the squalane internal standard, assuming similar response factors on the flame ionization detector.

3. Results

Sediment core GeoB9528-3 covers the last 192 ka and sedimentation rates varied between 1.2 and 9.5 cm/kyr (Figure 2). Levoglucosan was detected in all samples at concentrations varying from 0.2 to 2.8 ng/g dry weight sediment. Mannosan and galactosan were only present in trace amounts in 33 out of 187 samples and will not be discussed further. This is in agreement with the findings of Schreuder et al. (2018), who also detected mannosan and galactosan only in trace amounts in surface sediments close to our core location. Using sediment accumulation rates and dry bulk densities, we converted levoglucosan concentrations to accumulation rates. From 192 until 80 ka, the levoglucosan accumulation rate was relatively stable, with an average value of 1.6 ng · cm^{-2} · kyr^{-1} (Figure 3b). At 80 ka, levoglucosan accumulation rates increased to values around 4.0 ng · cm^{-2} · kyr^{-1}, followed by two peaks of 11.0 and 17.1 ng · cm^{-2} · kyr^{-1} at 57 and 55 ka, respectively. After approximately 50 ka, levoglucosan accumulation rates decreased again to values around 4.0 ng · cm^{-2} · kyr^{-1} and remained relatively constant until approximately 20 ka, after which levoglucosan accumulation decreased to values around 1.8 ng · cm^{-2} · kyr^{-1}.

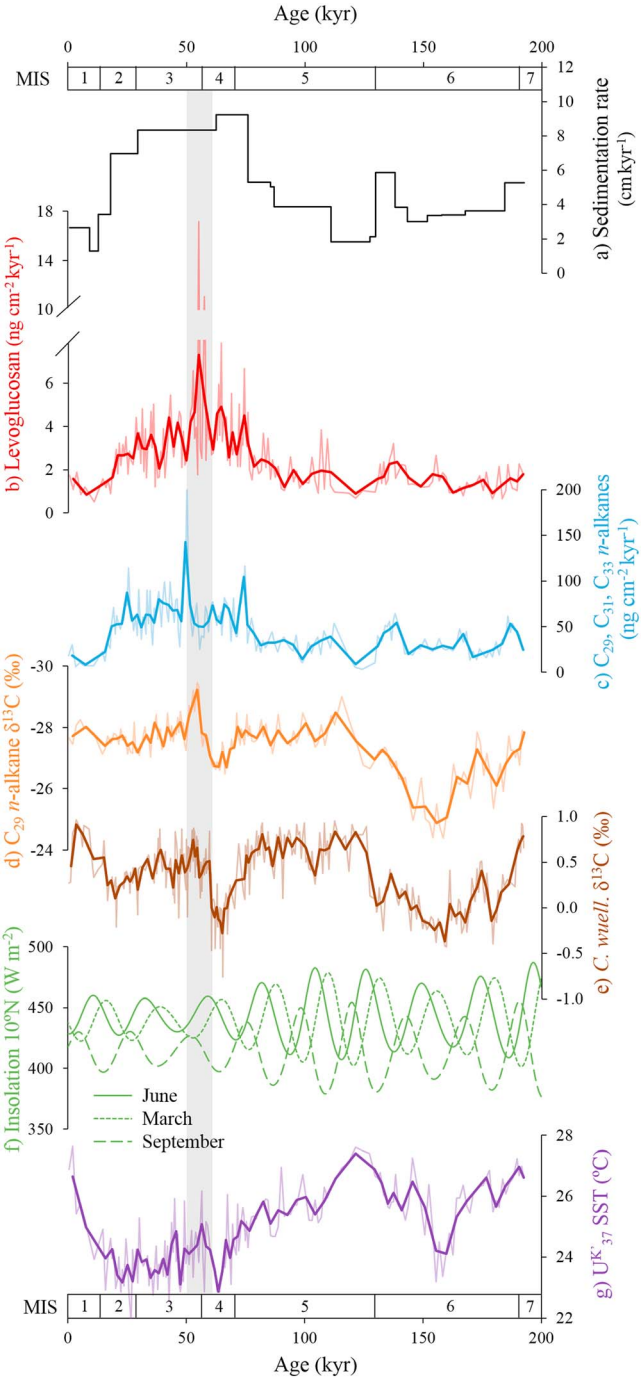

Figure 3. Comparison of geochemical records from core GeoB9528-3: (a) sedimentation rate; (b) levoglucosan accumulation rate; (c) accumulation rate of the sum of long-chain *n*-alkanes (C_{29}, C_{31}, and C_{33}); (d) $\delta^{13}C$ of the C_{29} *n*-alkane (Castañeda et al., 2009); (e) $\delta^{13}C$ of the benthic foraminifer *C. wuellerstorfi* (Castañeda et al., 2009); (f) insolation at 10°N for June, March, and September (Laskar et al., 2004); (g) sea surface temperature (SST) based on alkenones ($U^{K'}_{37}$; Castañeda et al., 2009). All isotope data are reported in delta notation (‰) against the VPDB standard. All thick lines in the graphs represent the smoothed data, three-point running mean. Marine isotope stages (MISs) are shown in the age axis. The grey shaded area represents the period of increased levoglucosan accumulation.

For comparison with the levoglucosan accumulation rate, we also determined accumulation rates of odd carbon numbered C_{29}-C_{33} *n*-alkanes, as a proxy for aeolian transported plant leaf waxes. Long-chain *n*-alkane concentrations varied between 2.3 and 37.7 ng/g dry weight sediment and, similar to levoglucosan, *n*-alkane concentrations were converted to accumulation rates. In the period between 192 and 80 ka, the *n*-alkane accumulation rate was approximately 32 ng · cm^{-2} · kyr^{-1} (Figure 3c). At 80 ka, the *n*-alkane accumulation rate increased to values around 65 ng · cm^{-2} · kyr^{-1} and remained relatively stable until approximately 20 ka, except for a peak at 50 ka, after which it decreased to approximately 20 ng · cm^{-2} · kyr^{-1} (Figure 3c).

4. Discussion

4.1. Factors Controlling Levoglucosan Accumulation Rates

Our levoglucosan record displays an increase in accumulation rate at 80 ka (Figure 3b), when the sedimentation rate as well as the long-chain *n*-alkane accumulation rate increased (Figures 3a and 3c). Since levoglucosan concentration remained constant at this time (Figure S1), it seems likely that increased levoglucosan accumulation rates were caused by an overall increase in sediment accumulation at this time rather than by increased biomass burning. Similarly, when levoglucosan accumulation rate decreased at 20 ka, sedimentation rate as well as the long-chain *n*-alkane accumulation rate also decreased and levoglucosan concentration remained constant (Figure S1), indicating that this decrease is also related to a change in sedimentation rate and not to biomass-burning changes. However, other variations in levoglucosan accumulation rate, such as the peaks at the onset of marine isotope stage (MIS) 3 (Figure 3b), do not coincide with changes in sedimentation rate and thus are interpreted to reflect variations in biomass burning.

Preservation conditions (i.e., oxygen exposure time; Hartnett et al., 1998) can markedly influence biomarker accumulation rates preserved in sedimentary archives (Sinninghe Damsté et al., 2002; Zonneveld et al., 2010). Indeed, Schreuder et al. (2018) found that levoglucosan is partially degraded at the sediment-water interface. However, this issue is only problematic when preservational conditions, for example, the time of oxygen exposure and/or the oxygen concentrations, have substantially changed over time. In that case, the levoglucosan record could be biased, leading to incorrect interpretation of the levoglucosan record in terms of the intensity of continental biomass burning. Changes in bottom water oxygen content can be inferred from Atlantic Meridional Ocean Circulation (AMOC) strength, since this governs the influx of North Atlantic Deep Water (NADW, oxygen-depleted) and Southern Ocean Water (SOW, oxygen-rich) to the core site. The AMOC strength can be reconstructed using the stable carbon isotope composition of the benthic foraminifer *Cibicidoides wuellerstorfi* ($\delta^{13}C_{benthic}$), since minima in $\delta^{13}C_{benthic}$ coincide with reductions in AMOC strength (Duplessy & Shackleton, 1985; Vidal et al., 1997), and thus an increased influx of oxygen-rich SOW to the core site. We see no direct correlation between levoglucosan accumulation rates and $\delta^{13}C_{benthic}$ (Figures 3b and 3e), ruling out a primary control by bottom water oxygen content. Furthermore, long-term degradation could have impacted the levoglucosan record. However, levoglucosan concentrations do not steadily decrease over the last 192 kyr (Figure S1).

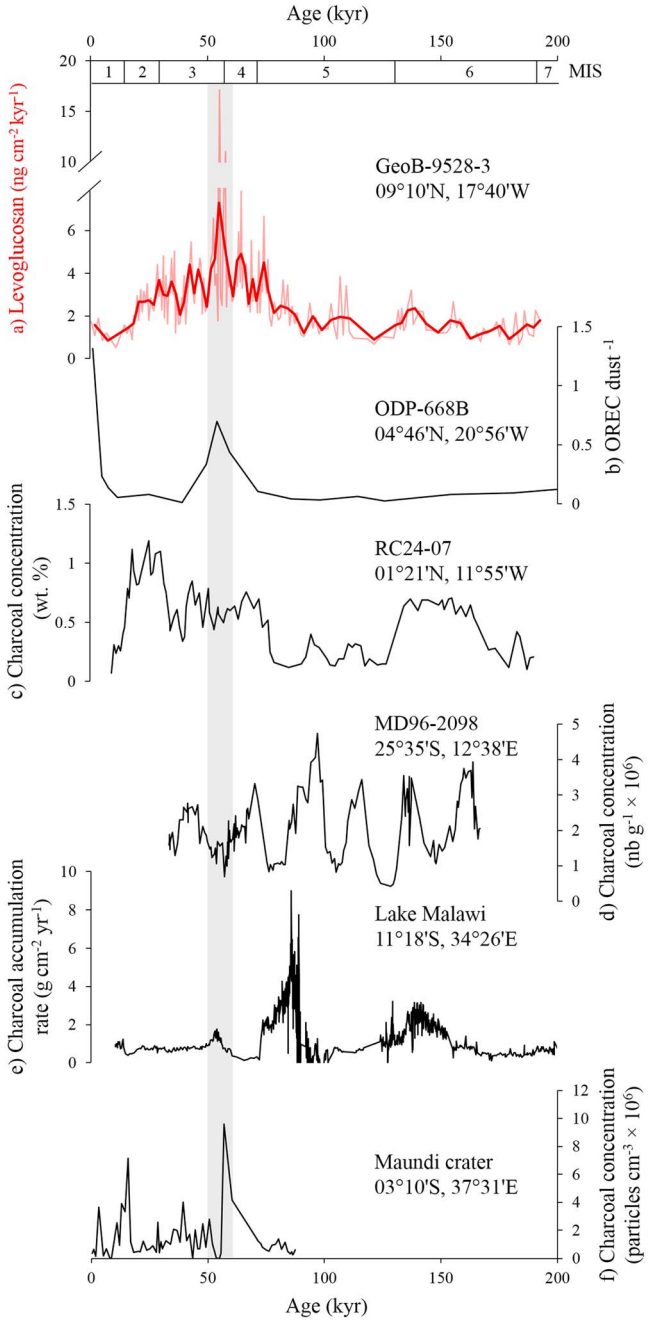

Figure 4. Comparison of the GeoB9528-3 levoglucosan accumulation rate with other records of fire-derived material from Africa: (a) levoglucosan accumulation rate (the thick line represents the smoothed data, three-point running mean) in marine core GeoB9528-3, (b) oxidation-resistant elemental carbon (OREC) as a ratio of the aeolian dust content in marine core ODP-668B (Bird & Cali, 1998; Bird & Cali, 2002), (c) elemental charcoal concentration (wt%) in marine sediment core RC24-07 (Verardo & Ruddiman, 1996), (d) microcharcoal (average length 4-200 μm) concentration in marine sediment core MD96-2098 (Daniau et al., 2013), (e) charcoal accumulation rate in lake core MAL05-1C (Ivory et al., 2018), and (f) charcoal concentration in Maundi crater (Schüler et al., 2012). Marine isotope stages (MISs) are shown in the age axis. The grey shaded area represents the period of increased levoglucosan accumulation. The location of the sites is indicated in Figure 1.

Therefore, we assume that preservation did not play a major role in influencing our levoglucosan record.

Other controlling factors on levoglucosan accumulation are the mode of transport and changes in source regions. Levoglucosan can be transported to the ocean by wind (e.g., Simoneit et al., 1999) or by rivers (e.g., Hunsinger et al., 2008). However, fluvial input from Africa is not likely at site GeoB9528-3 since it is located far offshore on the continental slope with no major rivers close by. Furthermore, the Branched and Isoprenoid Tetraether index values were on average only 0.06, signifying a low input of riverine transported organic matter (Hopmans et al., 2004; Schouten et al., 2013). Therefore, levoglucosan was likely transported to the core site by wind, in agreement with our previous study on the tropical North Atlantic (Schreuder et al., 2018). While we cannot fully rule out the possibility that some of the levoglucosan was transported from outside of the African continent, it seems likely that the predominant source is from continental Africa, since the position and direction of the AEJ likely remained constant during previous glacial and interglacial periods (Grousset et al., 1998). Therefore, the core GeoB9528-3 provides a continuous record of environmental changes in the forest-woodland-savanna boundary in the Guinean area of sub-Saharan Northwest Africa. No statistically significant relationship was found between levoglucosan concentrations and dust percentages in this core (Collins et al., 2013) over the last 60 ka ($R^2 = 0.015$, $p = 0.332$). Furthermore, there is a poor correlation between levoglucosan and long-chain *n*-alkane concentrations ($R^2 = 0.027$, $p = 0.026$). This suggests that there is no relationship between levoglucosan and aeolian input and therefore that levoglucosan trends are probably not related to changes in terrestrial input.

To further validate our levoglucosan record, we compared trends in levoglucosan accumulation rates with charcoal abundances in nearby marine sediment cores. In marine core ODP-668B (Figure 1), oxidation resistant elemental carbon (OREC) abundance was used as a proxy for wind-blown debris from biomass burning in the Northwest African sub-Sahara region (Bird & Cali, 1998; Bird & Cali, 2002). A sharp increase in OREC was found at the onset of MIS 3, coinciding with our levoglucosan peaks in core GeoB9528-3 at 57 and 55 ka (Figures 4a and 4b). In a marine core located further southeast (RC24-07; Figure 1), charcoal concentrations increased during glacials and do not coincide with changes in levoglucosan accumulation rate in our core (Figures 4a and 4c). However, the source area of fire-derived material in core RC24-07 is likely to be different than the one recorded in core GeoB9528-3. The agreement between the ODP-668B OREC record and our levoglucosan record implies that the levoglucosan record of GeoB9528-3 represents a continuous record of biomass burning in sub-Saharan Northwest Africa and that major biomass-burning events took place at the onset of MIS 3.

4.2. Factors Impacting the Fire History of Northwest Africa

Biomass burning is widespread in Africa and can be impacted by several factors including climate, vegetation, and human influence (e.g., Bond & Keeley, 2005; Bowman et al., 2009). Here we will discuss the impact of each of these factors on biomass burning in the Guinean area of sub-Saharan Northwest Africa.

4.2.1. Climate

The amount and seasonality of precipitation can impact biomass burning in the tropical savanna regions of Africa, by influencing tree and grass cover, which in turn has an impact on the fire regime (e.g., D'Onofrio et al., 2018; Lehmann et al., 2014). For example, in grass-dominated savanna areas on the African continent, increased precipitation antecedent to the fire season usually results in increased burned area, because of increased fuel buildup prior to the fire season (Abatzoglou et al., 2018; Archibald et al., 2009). In North Africa, hydrological conditions are controlled by the position of the tropical rainbelt over the African continent (Nicholson, 2009). The position of the tropical rainbelt is in turn influenced by precession-forced variability in summer insolation (e.g., deMenocal et al., 2000; Kuechler et al., 2018; Kutzbach & Liu, 1997). However, in sub-Saharan Northwest Africa, insolation is not of major influence on the position of the tropical rainbelt during the studied period (Castañeda et al., 2009). Here the position of the tropical rainbelt is predominantly controlled by the strength of the AMOC, since AMOC weakening causes sea surface temperature (SST) cooling in the North Atlantic region (Chang et al., 2008; Chiang et al., 2008) and a strengthening of the northeast trade winds (Chiang et al., 2008; Mulitza et al., 2008). These intensified trade winds, in combination with advection of cold air from the high latitudes, cause a southward shift of the tropical rainbelt (Chiang et al., 2008; Mulitza et al., 2008), leading to dry conditions in North Africa. Therefore, past hydrological conditions in sub-Saharan Northwest Africa were correlated to AMOC strength, which was reconstructed using $\delta^{13}C_{benthic}$, as previously done by Castañeda et al. (2009). The stable carbon isotope composition of long-chain *n*-alkanes (C_{29} and C_{31}) can provide information on vegetation composition (C_3 versus C_4 plants) from the savanna region (e.g., Castañeda et al., 2009). In tropical Africa, changes in hydrological conditions (wet season length and mean annual rainfall) are recognized as the dominant control on the large-scale distribution of C_3 versus C_4 vegetation on longer time scales. C_4 plants are enriched in $\delta^{13}C$ compared to C_3 plants (Collister et al., 1994), and in the Guinean area of sub-Saharan Northwest Africa, more C_4 vegetation reflects drier conditions (Castañeda et al., 2009; Kuechler et al., 2013). Therefore, past changes in C_3 versus C_4 vegetation, and related hydrological conditions, can be inferred from the *n*-alkane $\delta^{13}C$ record. We found no statistically significant relationship between levoglucosan accumulation rates and $\delta^{13}C_{benthic}$ ($R^2 = 0.00002$, $p = 0.958$) and a poor correlation between levoglucosan accumulation rates and $\delta^{13}C$ of the C_{29} *n*-alkane ($R^2 = 0.099$, $p < 0.05$). Thus, we do not have evidence that changes in African continental hydrology on glacial/interglacial timescales are of major influence on biomass burning in the savanna region in Northwest Africa. Air temperature could also affect fire in the Northwest African savanna region (Lehmann et al., 2014). For example, in warmer regions, fuels are more likely to cure, resulting in more frequent fire (Archibald et al., 2013). Direct records for air temperatures for the Northwest African savanna region on glacial/interglacial timescales are not available, and therefore, as general proxies for regional temperature, we used tropical North Atlantic SST (Castañeda et al., 2009) and June, March, and September insolation at 10°N (Laskar et al., 2004). We found that changes in tropical North Atlantic SST are not strongly correlated with changes in levoglucosan accumulation rates ($R^2 = 0.211$, $p < 0.05$), and we found no statistically significant relationship between levoglucosan accumulation rates and June, March, or September insolation ($R^2 = 0.0006$, $p = 0.746$; $R^2 = 0.0002$, $p = 0.847$; and $R^2 = 0.0004$, $p = 0.774$, respectively) over the last 192 kyr nor do they change when levoglucosan accumulation rate peaks around 57 and 55 ka (Figures 3b and 3f). This suggests that changes in regional temperature on glacial/interglacial timescales are also not the major influence on biomass burning in the savanna region of Northwest Africa.

4.2.2. Vegetation

Another factor that can impact biomass burning is vegetation composition and abundance. The stable carbon isotope composition of long-chain *n*-alkanes (C_{29} and C_{31}) can provide information on vegetation composition (C_3 versus C_4 plants) from the savanna region (e.g., Castañeda et al., 2009; Schefuß et al., 2004). Interestingly, there is no strong relationship between glacial/interglacial changes in $\delta^{13}C$ of the C_{29} *n*-alkane (Castañeda et al., 2009) and levoglucosan accumulation in core GeoB9528-3 over the last 192 ka ($R^2 = 0.099$, $p < 0.05$; Figures 3b and 3d). It thus seems that on longer (glacial/interglacial) timescales, biomass burning and vegetation composition in the savanna region of Northwest Africa are not coupled. This is in contrast with the general understanding that fire occurrence and vegetation composition are closely connected (e.g., Bond et al., 2005; Bond & Keeley, 2005; Lehmann et al., 2014). In Africa, the few available long-term (glacial/interglacial) fire studies found increased biomass burning during colder and wetter conditions, for

example, in Northwest Africa (Figure 4c; Verardo & Ruddiman, 1996) and in Southern Africa (Figure 4d; Daniau et al., 2013). This was related to increased fuel availability due to a shift in rainfall amount and seasonality and therefore increased biomass burning (Daniau et al., 2013). In the southern African tropics, extreme arid conditions resulted in decreased fire occurrence, related to insufficient vegetation to maintain substantial fires. Furthermore, a minor peak in charcoal accumulation rate occurred at approximately 50 ka, at the same time as the levoglucosan peaks in our record (Figure 4e; Cohen et al., 2007; Ivory et al., 2018). In equatorial East Africa, biomass burning played an important role in controlling the development and elevation of the ericaceous zone and the tree line on Mt Kilimanjaro (Figure 4f; Schüler et al., 2012). However, our record indicates that there may be a decoupling between vegetation composition and fire activity in the savanna region in Northwest Africa on glacial to interglacial time scales, while the two levoglucosan peaks at the onset of MIS 3 in our record coincide with a period of increased C_3 vegetation and wetter conditions (Figure 3d; Castañeda et al., 2009). We hypothesize that this increase in C_3 vegetation resulted in increased fuel load and biomass-burning activity, supported by earlier studies that have found increased fire activity during wetter climate conditions (e.g., Daniau et al., 2013).

4.2.3. Impact of Humans

Another factor may be the human influence on fire frequency in Africa, as suggested by Bird and Cali (1998) and found for the West Pacific-East Asian region (Thevenon et al., 2004) and Australia (Van Der Kaars et al., 2017). Indeed, humans can affect fire occurrence in Africa through manipulation of the frequency of ignition events, the timing of ignition events in the year, and the connectivity of the fuel bed by changing the proportion of cultivated and grazed land (Archibald et al., 2010; Archibald et al., 2012). However, it has been proven to be difficult to assess when humans started to influence biomass burning (Archibald et al., 2012). Archeological evidence suggested that the first unequivocal evidence for human fire use was around 300–200 ka, but evidence is sporadic for this time period (e.g., Karkanas et al., 2007). Other evidence has shown that the routine domestic use of fire began around 100–50 ka (Bowman et al., 2009), and hunter-gatherers used fire for hunting activities and to reduce fuels beginning tens of thousands of years ago (Pyne, 2011).

The earliest remains of fully modern humans date to 195 ka and originate from Ethiopia (McDougall et al., 2005), and fossils displaying some features of early anatomical modernity are dated to 315 ka, in Morocco (Hublin et al., 2017). Northwest Africa played a key role in the dispersal of anatomically modern humans (e.g., Osborne et al., 2008; Stringer, 2000), which originated in sub-Saharan Africa and had to pass through/settle in the savanna region. A major dispersal period occurred between 100 and 130 ka (Osborne et al., 2008; Stringer, 2000), and a second major dispersal period of hominins out of Africa occurred around 40–60 ka (Forster et al., 2001; Mellars, 2006; Stringer, 2000). Interestingly, the latter dispersal coincided with the two major peaks in levoglucosan accumulation rate at 57 and 55 ka (Figure 3b). This suggests that there might be a relationship between the second dispersal of hominids out of Africa and fire occurrence in the Guinean area of sub-Saharan Northwest Africa. As inferred by Castañeda et al. (2009), this region became wetter and C_3 vegetation increased at that time (Figure 3d) and therefore was more hospitable for humans allowing them to disperse into Europe and Asia. Furthermore, this period coincides with the boundary between the Middle and Upper Paleolithic, which is generally associated with a change in the social and technological behavior of humans (e.g., Rebollo et al., 2011). The increased fuel load together with the human occupation of the savanna region may thus have led to increased use of fire and increased levels of biomass burning. Only a minor increase in levoglucosan accumulation rate was observed at around 100–130 ka, though conditions were also more hospitable then (Castañeda et al., 2009) and humans likely crossed or settled in this region. However, there was less C_3 vegetation during this time than around 40–60 ka, and also, the use of fire was probably much less common than around 40–60 ka, as routine domestic use of fire began only around 100–50 ka (Bowman et al., 2009).

5. Conclusions

We reconstructed biomass burning in the Guinean area of sub-Saharan Northwest Africa for the last 192 kyr by using the accumulation rate of the fire biomarker levoglucosan in a marine core from the Guinean margin. Changes in levoglucosan accumulation rate are probably not related to changes in input of terrestrial material or changes in preservation conditions. Therefore, the levoglucosan record represents a continuous record of biomass burning in the sub-Saharan savanna region of Northwest Africa. Comparison with other

records shows that glacial/interglacial changes in regional climate and vegetation composition did not exert the dominant influence on biomass burning over the last 192 kyr in this area. In contrast, the two biomass-burning maxima at the onset of MIS 3 are likely related to a strong increase in C_3 vegetation and human occupation of the savanna region around 40–60 ka. The strong C_3 expansion likely led to increased fuel loads and increased levels of (human-induced) biomass burning in the sub-Saharan savanna region of Northwest Africa.

Acknowledgments
We thank members of the University of Bremen Geosciences Department and the Center for Marine Environmental Sciences for samples from GeoB9528-3. We thank Raquel A. Lopes dos Santos for laboratory assistance. We thank two anonymous reviewers and Editor James Russell for useful comments, which improved the manuscript. The research was funded by the Netherlands Organization for Scientific Research (NWO; project 824.14.001). S. S. and J. S. S. D. are supported by the Netherlands Earth System Science Center (NESSC) funded by the Dutch Ministry of Science, Culture and Education. The data supporting the conclusions is available in the supporting information.

References

Abatzoglou, J. T., Williams, A. P., Boschetti, L., Zubkova, M., & Kolden, C. A. (2018). Global patterns of interannual climate–fire relationships. *Global Change Biology*, *24*(11), 5164–5175. https://doi.org/10.1111/gcb.14405

Archibald, S., Lehmann, C. E., Gómez-Dans, J. L., & Bradstock, R. A. (2013). Defining pyromes and global syndromes of fire regimes. *Proceedings of the National Academy of Sciences*, 201211466.

Archibald, S., Roy, D. P., van Wilgen, B. W., & Scholes, R. J. (2009). What limits fire? An examination of drivers of burnt area in southern Africa. *Global Change Biology*, *15*(3), 613–630. https://doi.org/10.1111/j.1365-2486.2008.01754.x

Archibald, S., Scholes, R., Roy, D., Roberts, G., & Boschetti, L. (2010). Southern African fire regimes as revealed by remote sensing. *International Journal of Wildland Fire*, *19*(7), 861–878. https://doi.org/10.1071/WF10008

Archibald, S., Staver, A. C., & Levin, S. A. (2012). Evolution of human-driven fire regimes in Africa. *Proceedings of the National Academy of Sciences*, *109*, 847–852.

Battistel, D., Argiriadis, E., Kehrwald, N., Spigariol, M., Russell, J. M., & Barbante, C. (2017). Fire and human record at Lake Victoria, East Africa, during the Early Iron Age: Did humans or climate cause massive ecosystem changes? *The Holocene*, *27*(7), 997–1007. https://doi.org/10.1177/0959683616678466

Bird, M., & Cali, J. (1998). A million-year record of fire in sub-Saharan Africa. *Nature*, *394*(6695), 767–769. https://doi.org/10.1038/29507

Bird, M. I., & Cali, J. A. (2002). A revised high-resolution oxygen-isotope chronology for ODP-668B: Implications for Quaternary biomass burning in Africa. *Global and Planetary Change*, *33*(1-2), 73–76. https://doi.org/10.1016/S0921-8181(02)00062-0

Blaauw, M., & Christen, J. A. (2011). Flexible paleoclimate age-depth models using an autoregressive gamma process. *Bayesian Analysis*, *6*, 457–474.

Bond, W. J., & Keeley, J. E. (2005). Fire as a global 'herbivore': The ecology and evolution of flammable ecosystems. *Trends in Ecology & Evolution*, *20*(7), 387–394. https://doi.org/10.1016/j.tree.2005.04.025

Bond, W. J., Woodward, F. I., & Midgley, G. F. (2005). The global distribution of ecosystems in a world without fire. *New Phytologist*, *165*, 525–538.

Bowman, D. M., Balch, J. K., Artaxo, P., Bond, W. J., Carlson, J. M., Cochrane, M. A., et al. (2009). Fire in the Earth system. *Science*, *324*(5926), 481–484. https://doi.org/10.1126/science.1163886

Castañeda, I. S., Mulitza, S., Schefuß, E., Lopes dos Santos, R. A., Sinninghe Damsté, J. S., & Schouten, S. (2009). Wet phases in the Sahara/Sahel region and human migration patterns in North Africa. *Proceedings of the National Academy of Sciences*, *106*, 20,159–20,163.

Chang, P., Zhang, R., Hazeleger, W., Wen, C., Wan, X., Ji, L., et al. (2008). Oceanic link between abrupt changes in the North Atlantic Ocean and the African monsoon. *Nature Geoscience*, *1*(7), 444–448. https://doi.org/10.1038/ngeo218

Chiang, J. C., Cheng, W., & Bitz, C. M. (2008). Fast teleconnections to the tropical Atlantic sector from Atlantic thermohaline adjustment. *Geophysical Research Letters*, *35*, L07704. https://doi.org/10.1029/2008GL033292

Cohen, A. S., Stone, J. R., Beuning, K. R., Park, L. E., Reinthal, P. N., Dettman, D., et al. (2007). Ecological consequences of early Late Pleistocene megadroughts in tropical Africa. *Proceedings of the National Academy of Sciences*, *104*(42), 16,422–16,427. https://doi.org/10.1073/pnas.0703873104

Collins, J. A., Govin, A., Mulitza, S., Heslop, D., Zabel, M., Hartmann, J., et al. (2013). Abrupt shifts of the Sahara-Sahel boundary during Heinrich stadials. *Climate of the Past*, *9*(3), 1181–1191. https://doi.org/10.5194/cp-9-1181-2013

Collister, J. W., Rieley, G., Stern, B., Eglinton, G., & Fry, B. (1994). Compound-specific $\delta^{13}C$ analyses of leaf lipids from plants with differing carbon dioxide metabolisms. *Organic Geochemistry*, *21*(6-7), 619–627. https://doi.org/10.1016/0146-6380(94)90008-6

Daniau, A.-L., Goñi, M. F. S., Martinez, P., Urrego, D. H., Bout-Roumazeilles, V., Desprat, S., & Marlon, J. R. (2013). Orbital-scale climate forcing of grassland burning in southern Africa. *Proceedings of the National Academy of Sciences*, *110*, 5069–5073.

deMenocal, P., Ortiz, J., Guilderson, T., Adkins, J., Sarnthein, M., Baker, L., & Yarusinsky, M. (2000). Abrupt onset and termination of the African Humid Period: Rapid climate responses to gradual insolation forcing. *Quaternary Science Reviews*, *19*(1-5), 347–361. https://doi.org/10.1016/S0277-3791(99)00081-5

deMenocal, P. B. (1995). Plio-pleistocene African climate. *Science*, *270*(5233), 53–59. https://doi.org/10.1126/science.270.5233.53

D'Onofrio, D., von Hardenberg, J., & Baudena, M. (2018). Not only trees: Grasses determine African tropical biome distributions via water limitation and fire. *Global Ecology and Biogeography*, *27*(6), 714–725. https://doi.org/10.1111/geb.12735

Duplessy, J.-C., & Shackleton, N. J. (1985). Response of global deep-water circulation to Earth's climatic change 135,000–107,000 years ago. *Nature*, *316*(6028), 500–507. https://doi.org/10.1038/316500a0

Dupont, L., & Schefuß, E. (2018). The roles of fire in Holocene ecosystem changes of West Africa. *Earth and Planetary Science Letters*, *481*, 255–263. https://doi.org/10.1016/j.epsl.2017.10.049

Elias, V. O., Simoneit, B. R., Cordeiro, R. C., & Turcq, B. (2001). Evaluating levoglucosan as an indicator of biomass burning in Carajas, Amazonia: A comparison to the charcoal record. *Geochimica et Cosmochimica Acta*, *65*(2), 267–272. https://doi.org/10.1016/S0016-7037(00)00522-6

Forster, P., Torroni, A., Renfrew, C., & Röhl, A. (2001). Phylogenetic star contraction applied to Asian and Papuan mtDNA evolution. *Molecular Biology and Evolution*, *18*(10), 1864–1881. https://doi.org/10.1093/oxfordjournals.molbev.a003728

Fraser, M. P., & Lakshmanan, K. (2000). Using levoglucosan as a molecular marker for the long-range transport of biomass combustion aerosols. *Environmental Science & Technology*, *34*(21), 4560–4564. https://doi.org/10.1021/es991229l

Fu, P., Kawamura, K., & Miura, K. (2011). Molecular characterization of marine organic aerosols collected during a round-the-world cruise. *Journal of Geophysical Research*, *116*, D13302. https://doi.org/10.1029/2011JD015604

García, M. I., Drooge, B. L. V., Rodríguez, S., & Alastuey, A. (2017). Speciation of organic aerosols in the Saharan Air Layer and in the free troposphere westerlies. *Atmospheric Chemistry and Physics*, *17*(14), 8939–8958. https://doi.org/10.5194/acp-17-8939-2017

Grousset, F., Parra, M., Bory, A., Martinez, P., Bertrand, P., Shimmield, G., & Ellam, R. (1998). Saharan wind regimes traced by the Sr–Nd isotopic composition of subtropical Atlantic sediments: Last glacial maximum vs today. *Quaternary Science Reviews*, *17*(4-5), 395–409. https://doi.org/10.1016/S0277-3791(97)00048-6

Hartnett, H. E., Keil, R. G., Hedges, J. I., & Devol, A. H. (1998). Influence of oxygen exposure time on organic carbon preservation in continential margin sediments. *Nature*, *391*(6667), 572–572, 575. https://doi.org/10.1038/35351

Hawthorne, D., Mustaphi, C. J. C., Aleman, J. C., Blarquez, O., Colombaroli, D., Daniau, A.-L., et al. (2017). Global Modern Charcoal Dataset (GMCD): A tool for exploring proxy-fire linkages and spatial patterns of biomass burning. *Quaternary International*, *488*, 3–17.

Hopmans, E. C., Weijers, J. W., Schefuß, E., Herfort, L.,Damsté, J. S. S., & Schouten, S. (2004). A novel proxy for terrestrial organic matter in sediments based on branched and isoprenoid tetraether lipids. *Earth and Planetary Science Letters*, *224*(1-2), 107–116.

Hu, Q.-H., Xie, Z.-Q., Wang, X.-M., Kang, H., & Zhang, P. (2013). Levoglucosan indicates high levels of biomass burning aerosols over oceans from the Arctic to Antarctic. *Scientific Reports*, *3*(1), 3119. https://doi.org/10.1038/srep03119

Hublin, J.-J., Ben-Ncer, A., Bailey, S. E., Freidline, S. E., Neubauer, S., Skinner, M. M., et al. (2017). New fossils from Jebel Irhoud, Morocco and the pan-African origin of Homo sapiens. *Nature*, *546*(7657), 289–292. https://doi.org/10.1038/nature22336

Hunsinger, G. B., Mitra, S., Warrick, J. A., & Alexander, C. R. (2008). Oceanic loading of wildfire-derived organic compounds from a small mountainous river. *Journal of Geophysical Research*, *113*, G02007. https://doi.org/10.1029/2007JG000476

Iinuma, Y., Keywood, M., & Herrmann, H. (2016). Characterization of primary and secondary organic aerosols in Melbourne airshed: The influence of biogenic emissions, wood smoke and bushfires. *Atmospheric Environment*, *130*, 54–63. https://doi.org/10.1016/j.atmosenv.2015.12.014

Ivory, S. J., Lézine, A. M., Vincens, A., & Cohen, A. S. (2018). Waxing and waning of forests: Late Quaternary biogeography of southeast Africa. *Global Change Biology*, *24*(7), 2939–2951. https://doi.org/10.1111/gcb.14150

Karkanas, P., Shahack-Gross, R., Ayalon, A., Bar-Matthews, M., Barkai, R., Frumkin, A., et al. (2007). Evidence for habitual use of fire at the end of the lower Paleolithic: Site-formation processes at Qesem Cave, Israel. *Journal of Human Evolution*, *53*(2), 197–212. https://doi.org/10.1016/j.jhevol.2007.04.002

Koopmans, M. P., Köster, J., Van Kaam-Peters, H. M., Kenig, F., Schouten, S., Hartgers, W. A., et al. (1996). Diagenetic and catagenetic products of isorenieratene: Molecular indicators for photic zone anoxia. *Geochimica et Cosmochimica Acta*, *60*(22), 4467–4496. https://doi.org/10.1016/S0016-7037(96)00238-4

Kuechler, R., Schefuß, E., Beckmann, B., Dupont, L., & Wefer, G. (2013). NW African hydrology and vegetation during the Last Glacial cycle reflected in plant-wax-specific hydrogen and carbon isotopes. *Quaternary Science Reviews*, *82*, 56–67. https://doi.org/10.1016/j.quascirev.2013.10.013

Kuechler, R. R., Dupont, L. M., & Schefuß, E. (2018). Hybrid insolation forcing of Pliocene monsoon dynamics in West Africa. *Climate of the Past*, *14*(1), 73–84. https://doi.org/10.5194/cp-14-73-2018

Kuo, L.-J., Herbert, B. E., & Louchouarn, P. (2008). Can levoglucosan be used to characterize and quantify char/charcoal black carbon in environmental media? *Organic Geochemistry*, *39*(10), 1466–1478. https://doi.org/10.1016/j.orggeochem.2008.04.026

Kuo, L.-J., Louchouarn, P., & Herbert, B. E. (2011). Influence of combustion conditions on yields of solvent-extractable anhydrosugars and lignin phenols in chars: Implications for characterizations of biomass combustion residues. *Chemosphere*, *85*(5), 797–805. https://doi.org/10.1016/j.chemosphere.2011.06.074

Kutzbach, J. E., & Liu, Z. (1997). Response of the African monsoon to orbital forcing and ocean feedbacks in the middle Holocene. *Science*, *278*(5337), 440–443. https://doi.org/10.1126/science.278.5337.440

Laskar, J., Robutel, P., Joutel, F., Gastineau, M., Correia, A., & Levrard, B. (2004). A long-term numerical solution for the insolation quantities of the Earth. *Astronomy & Astrophysics*, *428*(1), 261–285. https://doi.org/10.1051/0004-6361:20041335

Lehmann, C. E., Anderson, T. M., Sankaran, M., Higgins, S. I., Archibald, S., Hoffmann, W. A., et al. (2014). Savanna vegetation-fire-climate relationships differ among continents. *Science*, *343*(6170), 548–552. https://doi.org/10.1126/science.1247355

Lisiecki, L. E., & Raymo, M. E. (2005). A Pliocene-Pleistocene stack of 57 globally distributed benthic δ18O records. *Paleoceanography*, *20*, PA1003. https://doi.org/10.1029/2004PA001071

Lisiecki, L. E., & Stern, J. V. (2016). Regional and global benthic δ18O stacks for the last glacial cycle. *Paleoceanography*, *31*, 1368–1394. https://doi.org/10.1002/2016PA003002

Lopes dos Santos, R. A., Prange, M., Castañeda, I. S., Schefuß, E., Mulitza, S., Schulz, M., et al. (2010). Glacial–interglacial variability in Atlantic meridional overturning circulation and thermocline adjustments in the tropical North Atlantic. *Earth and Planetary Science Letters*, *300*(3-4), 407–414. https://doi.org/10.1016/j.epsl.2010.10.030

Marlon, J. R., Kelly, R., Daniau, A.-L., Vannière, B., Power, M. J., Bartlein, P., et al. (2016). Reconstructions of biomass burning from sediment charcoal records to improve data-model comparisons. *Biogeosciences*, *13*(11), 3225–3244. https://doi.org/10.5194/bg-13-3225-2016

McDougall, I., Brown, F. H., & Fleagle, J. G. (2005). Stratigraphic placement and age of modern humans from Kibish, Ethiopia. *Nature*, *433*(7027), 733–736. https://doi.org/10.1038/nature03258

Mellars, P. (2006). Going east: New genetic and archaeological perspectives on the modern human colonization of Eurasia. *Science*, *313*(5788), 796–800. https://doi.org/10.1126/science.1128402

Miller, D. R., Castañeda, I. S., Bradley, R. S., & MacDonald, D. (2017). Local and regional wildfire activity in central Maine (USA) during the past 900 years. *Journal of Paleolimnology*, *58*(4), 455–466. https://doi.org/10.1007/s10933-017-0002-z

Mochida, M., Kawamura, K., Umemoto, N., Kobayashi, M., Matsunaga, S., Lim, H. J., et al. (2003). Spatial distributions of oxygenated organic compounds (dicarboxylic acids, fatty acids, and levoglucosan) in marine aerosols over the western Pacific and off the coast of East Asia: Continental outflow of organic aerosols during the ACE-Asia campaign. *Journal of Geophysical Research*, *108*(D23), 8638. https://doi.org/10.1029/2002JD003249

Monteiro, A., Gouveia, S., Scotto, M., Sorte, S., Gama, C., Gianelle, V. L., et al. (2018). Investigating PM10 episodes using levoglucosan as tracer. *Air Quality, Atmosphere and Health*, *11*(1), 61–68. https://doi.org/10.1007/s11869-017-0521-9

Mouillot, F., & Field, C. B. (2005). Fire history and the global carbon budget: A 1 × 1 fire history reconstruction for the 20th century. *Global Change Biology*, *11*(3), 398–420. https://doi.org/10.1111/j.1365-2486.2005.00920.x

Mulitza, S., Prange, M., Stuut, J. B., Zabel, M., von Dobeneck, T., Itambi, A. C., et al. (2008). Sahel megadroughts triggered by glacial slowdowns of Atlantic meridional overturning. *Paleoceanography*, *23*, PA4206. https://doi.org/10.1029/2008PA001637

Nicholson, S. E. (2009). A revised picture of the structure of the "monsoon" and land ITCZ over West Africa. *Climate Dynamics*, *32*(7-8), 1155–1171. https://doi.org/10.1007/s00382-008-0514-3

Osborne, A. H., Vance, D., Rohling, E. J., Barton, N., Rogerson, M., & Fello, N. (2008). A humid corridor across the Sahara for the migration of early modern humans out of Africa 120,000 years ago. *Proceedings of the National Academy of Sciences*, *105*, 16,444–16,447.

Peters, K. E., Walters, C. C., & Moldowan, J. M. (2005). *The biomarker guide*. Cambridge, UK: Cambridge University Press.
Pyne, S. J. (2011). *Fire: A brief history*. Seattle, WA: University of Washington Press.
Rebollo, N. R., Weiner, S., Brock, F., Meignen, L., Goldberg, P., Belfer-Cohen, A., et al. (2011). New radiocarbon dating of the transition from the Middle to the Upper Paleolithic in Kebara Cave, Israel. *Journal of Archaeological Science*, *38*(9), 2424–2433. https://doi.org/10.1016/j.jas.2011.05.010
Schefuß, E., Schouten, S., Jansen, J. F., & Damsté, J. S. S. (2003). African vegetation controlled by tropical sea surface temperatures in the mid-Pleistocene period. *Nature*, *422*(6930), 418–421. https://doi.org/10.1038/nature01500
Schefuß, E., Versteegh, G. J., Jansen, J., & Sinninghe Damsté, J. (2004). Lipid biomarkers as major source and preservation indicators in SE Atlantic surface sediments. *Deep Sea Research Part I: Oceanographic Research Papers*, *51*(9), 1199–1228. https://doi.org/10.1016/j.dsr.2004.05.002
Schouten, S., Hopmans, E. C., Rosell-Melé, A., Pearson, A.,Adam, P., Bauersachs, T., et al.(2013). An interlaboratory study of TEX86 and BIT analysis of sediments, extracts, and standard mixtures. *Geochemistry, Geophysics, Geosystems*, *14*, 5263–5285. https://doi.org/10.1002/2013GC004904
Schreuder, L. T., Hopmans, E. C., Stuut, J.-B. W., Damsté, J. S. S., & Schouten, S. (2018). Transport and deposition of the fire biomarker levoglucosan across the tropical North Atlantic Ocean. *Geochimica et Cosmochimica Acta*, *227*, 171–185. https://doi.org/10.1016/j.gca.2018.02.020
Schüler, L., Hemp, A., Zech, W., & Behling, H. (2012). Vegetation, climate and fire-dynamics in East Africa inferred from the Maundi crater pollen record from Mt Kilimanjaro during the last glacial–interglacial cycle. *Quaternary Science Reviews*, *39*, 1–13. https://doi.org/10.1016/j.quascirev.2012.02.003
Shafizadeh, F., Furneaux, R. H., Cochran, T. G., Scholl, J. P., & Sakai, Y. (1979). Production of levoglucosan and glucose from pyrolysis of cellulosic materials. *Journal of Applied Polymer Science*, *23*(12), 3525–3539. https://doi.org/10.1002/app.1979.070231209
Shanahan, T. M., Hughen, K. A., McKay, N. P., Overpeck, J. T., Scholz, C. A., Gosling, W. D., et al. (2016). CO_2 and fire influence tropical ecosystem stability in response to climate change. *Scientific Reports*, *6*(1), 29,587. https://doi.org/10.1038/srep29587
Simoneit, B. R., & Elias, V. O. (2000). Organic tracers from biomass burning in atmospheric particulate matter over the ocean. *Marine Chemistry*, *69*(3-4), 301–312. https://doi.org/10.1016/S0304-4203(00)00008-6
Simoneit, B. R., Schauer, J. J., Nolte, C., Oros, D. R., Elias, V. O., Fraser, M., et al. (1999). Levoglucosan, a tracer for cellulose in biomass burning and atmospheric particles. *Atmospheric Environment*, *33*(2), 173–182. https://doi.org/10.1016/S1352-2310(98)00145-9
Sinninghe Damsté, J. S., Rijpstra, W. I. C., & Reichart, G.-J. (2002). The influence of oxic degradation on the sedimentary biomarker record II. Evidence from Arabian Sea sediments. *Geochimica et Cosmochimica Acta*, *66*(15), 2737–2754. https://doi.org/10.1016/S0016-7037(02)00865-7
Stringer, C. (2000). Palaeoanthropology: Coasting out of Africa. *Nature*, *405*(6782), 24–27. https://doi.org/10.1038/35011166
Thevenon, F., Bard, E., Williamson, D., & Beaufort, L. (2004). A biomass burning record from the West Equatorial Pacific over the last 360 ky: Methodological, climatic and anthropic implications. *Palaeogeography, Palaeoclimatology, Palaeoecology*, *213*(1-2), 83–99. https://doi.org/10.1016/S0031-0182(04)00364-5
Tobiszewski, M., & Namieśnik, J. (2012). PAH diagnostic ratios for the identification of pollution emission sources. *Environmental Pollution*, *162*, 110–119. https://doi.org/10.1016/j.envpol.2011.10.025
Vachula, R. S., Russell, J. M., Huang, Y., & Richter, N. (2018). Assessing the spatial fidelity of sedimentary charcoal size fractions as fire history proxies with a high-resolution sediment record and historical data. *Palaeogeography, Palaeoclimatology, Palaeoecology*, *508*, 166–175. https://doi.org/10.1016/j.palaeo.2018.07.032
Van Der Kaars, S., Miller, G. H., Turney, C. S., Cook, E. J., Nürnberg, D., Schönfeld, J., et al. (2017). Humans rather than climate the primary cause of Pleistocene megafaunal extinction in Australia. *Nature Communications*, *8*, 14142. https://doi.org/10.1038/ncomms14142
Verardo, D. J., & Ruddiman, W. F. (1996). Late Pleistocene charcoal in tropical Atlantic deep-sea sediments: Climatic and geochemical significance. *Geology*, *24*(9), 855–857. https://doi.org/10.1130/0091-7613(1996)024<0855:LPCITA>2.3.CO;2
Vidal, L., Labeyrie, L., Cortijo, E., Arnold, M., Duplessy, J., Michel, E., et al. (1997). Evidence for changes in the North Atlantic Deep Water linked to meltwater surges during the Heinrich events. *Earth and Planetary Science Letters*, *146*(1-2), 13–27. https://doi.org/10.1016/S0012-821X(96)00192-6
Wakeham, S. G., Schaffner, C., & Giger, W. (1980). Poly cyclic aromatic hydrocarbons in Recent lake sediments—II. Compounds derived from biogenic precursors during early diagenesis. *Geochimica et Cosmochimica Acta*, *44*, 415–429.
Wang, Q., Shao, M., Liu, Y., William, K., Paul, G., Li, X., et al. (2007). Impact of biomass burning on urban air quality estimated by organic tracers: Guangzhou and Beijing as cases. *Atmospheric Environment*, *41*(37), 8380–8390. https://doi.org/10.1016/j.atmosenv.2007.06.048
Whitlock, C., Higuera, P. E., McWethy, D. B., & Briles, C. E. (2010). Paleoecological perspectives on fire ecology: Revisiting the fire-regime concept. *The Open Ecology Journal*, *3*(2), 6–23. https://doi.org/10.2174/1874213001003020006
Whitlock, C., & Larsen, C. (2002). Charcoal as a fire proxy. In J. P. Smol, H. J. B. Birks, W. M. Last, R. S. Bradly, & K. Alverson (Eds.), *Tracking environmental change using lake sediments* (pp. 75–97). Dordrecht, The Netherlands: Springer.
Yunker, M. B., Macdonald, R. W., Vingarzan, R., Mitchell, R. H., Goyette, D., & Sylvestre, S. (2002). PAHs in the Fraser River basin: A critical appraisal of PAH ratios as indicators of PAH source and composition. *Organic Geochemistry*, *33*(4), 489–515. https://doi.org/10.1016/S0146-6380(02)00002-5
Zonneveld, K., Versteegh, G., Kasten, S., Eglinton, T. I., Emeis, K.-C., Huguet, C., et al. (2010). Selective preservation of organic matter in marine environments: Processes and impact on the sedimentary record. *Biogeosciences*, *7*(2), 483–511. https://doi.org/10.5194/bg-7-483-2010